The effect of nitrogen incorporation in boron carbide and iridium thin films

Massahi, S.; Christensen, F. E.; Ferreira, D. D.M.; Dalampiras, P.; Svendsen, S.; Jafari, A.

Published in:
Space Telescopes and Instrumentation 2018: Ultraviolet to Gamma Ray

Link to article, DOI:
10.1117/12.2311622

Publication date:
2018

Document Version
Publisher's PDF, also known as Version of record

The effect of nitrogen incorporation in boron carbide and iridium thin films

S. Massahi, F. E. Christensen, D. D. M. Ferreira, P. Dalampiras, S. Svendsen, et al.

S. Massahi, F. E. Christensen, D. D. M. Ferreira, P. Dalampiras, S. Svendsen, A. Jafari, "The effect of nitrogen incorporation in boron carbide and iridium thin films," Proc. SPIE 10699, Space Telescopes and Instrumentation 2018: Ultraviolet to Gamma Ray, 106993Y (6 July 2018); doi: 10.1117/12.2311622

SPIE.

Event: SPIE Astronomical Telescopes + Instrumentation, 2018, Austin, Texas, United States

The effect of nitrogen incorporation in boron carbide and iridium thin films

S. Massahi, F.E. Christensen, D.D.M. Ferreira, P. Dalampiras, S. Svendsen and A. Jafari

DTU Space, Elektrovej 327, Kgs. Lyngby, Denmark;

ABSTRACT

Thin film coated mirrors enable pioneering observations of X-rays and soft gamma rays. The performance of the reflective mirrors is key in expanding knowledge of the hot and energetic Universe.
A critical part of maturing the optics technology is firstly, to establish a smooth surface and interface of the selected materials and, secondly, to obtain an in-depth understanding of the contamination in the thin films and ultimately, to ensure long-term stability.
The aim of this study is to investigate the chemical composition, roughness and stability of boron carbide and iridium thin films and the effects of nitrogen incorporation.

Keywords: Reactive sputtering, XPS, Athena, Silicon Pore Optics (SPO), Multilayer Deposition, DC Magnetron Sputtering, XRR, X-ray Optics

1. INTRODUCTION

Excellent thin films are crucial in advancing the performance and throughput of future X-ray optics missions. The increasing demand from the science community for mapping and exploring the hot and energetic Universe pushes the technology development. Several X-ray missions are under concept review and others are selected for flight, here-under Athena[1], an X-ray observatory selected by ESA as their X-ray astronomy flagship. Furthermore, other mission concepts such as LYNX[2] the High-Energy X-ray Probe (HEX-P)[3] are under considerations. These missions shall collect photons in a wide energy band, some from 100 eV - 12 keV and others from 2 keV - 200 keV. As a large collecting area is required to fulfill the science requirements, focusing optics are decisive. Focusing optics take advantage of thin films to increase the effective area of the telescope.
Simulations show that in the 100 eV - 12 keV energy range, iridium and boron carbide thin films have excellent reflective properties[4,5]. In 2016 we showed long term stability of Cr/Ir/B_4C trilayer films from 8.047 keV reflectivity scans[6]. Recently, we have observed instability of boron carbide in terms of composition variation when exposed to ambient[7].
In this article we investigate single films of boron carbide and iridium deposited non-reactively and reactively. We will map the potential chemical states in boron carbide and iridium through X-ray photo-electron spectroscopy. In addition we investigate the effect of introducing nitrogen in the sputtering process causing boron carbide to react with the nitrogen, ultimately, producing boron nitride and carbon nitride[8]. We are investigating several nitrogen/argon gas fractions to determine the nitrogen incorporation in the thin films and the potential insusceptibility to oxygen incorporation after film deposition.

2. EXPERIMENTAL

2.1 Sample preparation

The thin films discussed in this article were deposited on silicon pieces, referred to as witness samples in this article, of dimension: 70 mm x 10 mm x ∼0.75 mm. The pieces originate from dicing 300 mm P/boron doped double side polished silicon wafers. However, as a result of the dicing process, contamination was observed on the surface of the silicon. This was observed through Atomic Force Microscope (AFM) characterization, performed at two spots on the surface of a witness sample, illustrated in figure 1. The images in figure 2 illustrate the surface of the uncleaned witness samples. We presumed the contamination composition was organic, based on

Further author information: (Send correspondence to S. Massahi)
S. Massahi: E-mail: sonmas@space.dtu.dk, Telephone: +45 31 24 14 56

Space Telescopes and Instrumentation 2018: Ultraviolet to Gamma Ray, edited by Jan-Willem A. den Herder, Shouleh Nikzad, Kazuhiro Nakazawa, Proc. of SPIE Vol. 10699, 106993Y · © 2018 SPIE
CCC code: 0277-786X/18/$18 · doi: 10.1117/12.2311622

experience[9]. As a result, we plasma cleaned the witness samples with the following parameters: O_2: 400 sccm, N_2: 70 sccm, power: 1000 W, duration: 10 min The outcome is presented in figure 3, illustrating a clean silicon surface. The RMS values presented in table 1 are calculated using a 1D-PSD included in the NanoScope software. The surface roughness improved by a factor of 10 by plasma cleaning the witness samples.

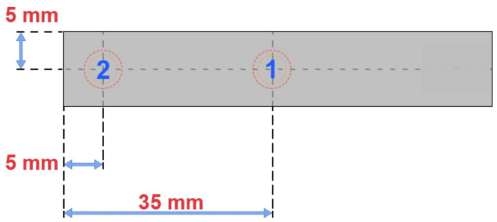

Figure 1: Illustration of scan area for spot 1 and spot 2.

Table 1: RMS values for uncleaned and cleaned silicon substrates.

		Spot 1	Spot 2
	Scan size (μ m)	σ (nm)	σ (nm)
Before plasma cleaning	1.00 × 1.00	0.53	2.07
	10.0 × 10.0	1.49	1.83
After plasma cleaning	1.00 × 1.00	0.20	0.20
	10.0 × 10.0	0.13	0.13

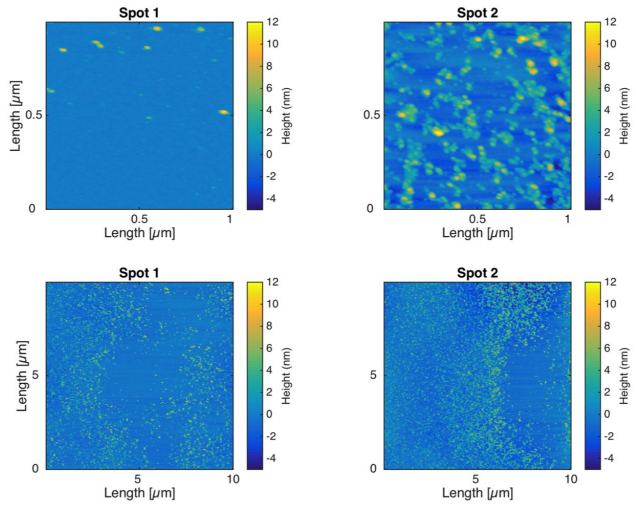

Figure 2: Images of the uncleaned witness sample surface. AFM measurements with scan-sizes: 1 x 1 μm and 10 x 10 μm.

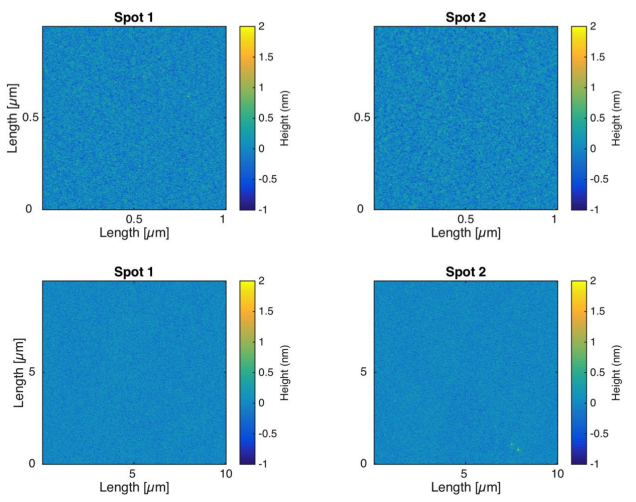

Figure 3: Images of the cleaned witness sample surface. AFM measurements with scan-sizes: 1 x 1 μm and 10 x 10 μm.

2.2 Thin film deposition

Single layers of iridium and boron carbide has been prepared using direct current magnetron sputtering, see figure 4. The base pressure of the chamber was lower than $2 \cdot 10^{-6}$ Torr to ensure a low amount of contamination in the chamber. The films were deposited in a pure argon and in a mixed argon/nitrogen atmosphere. To investigate the nitrogen incorporation in the thin films four different Ni/Ar gas fractions were studied (table 2). The total gas pressure in the chamber was kept between $2.9 - 3.1$ mTorr for film growth. The pressure range was due to thermal conditions during deposition.

The power density applied to the iridium and the boron carbide targets were 3.10 W/cm^2 and 5.17 W/cm^2, respectively. The target dimension is 508 mm in length and 38.1 mm in width. The substrate to target distance is $\sim$ 155 mm.

A 5 minutes presputtering was performed prior each process to remove contamination on the target surface and ensure a stable plasma.

Table 2: Total gas pressure of 3±0.1 mTorr. $Ni_{flow} = Ar_{flow}(\frac{x}{1-x})$, where x is the gas fraction.

Process #	Ar flow rate (sccm)	N_2 flow rate (sccm)	Gas fraction %
1	96	0	0
2	88	4.6	5
3	85	9.4	10
4	81	14.3	15

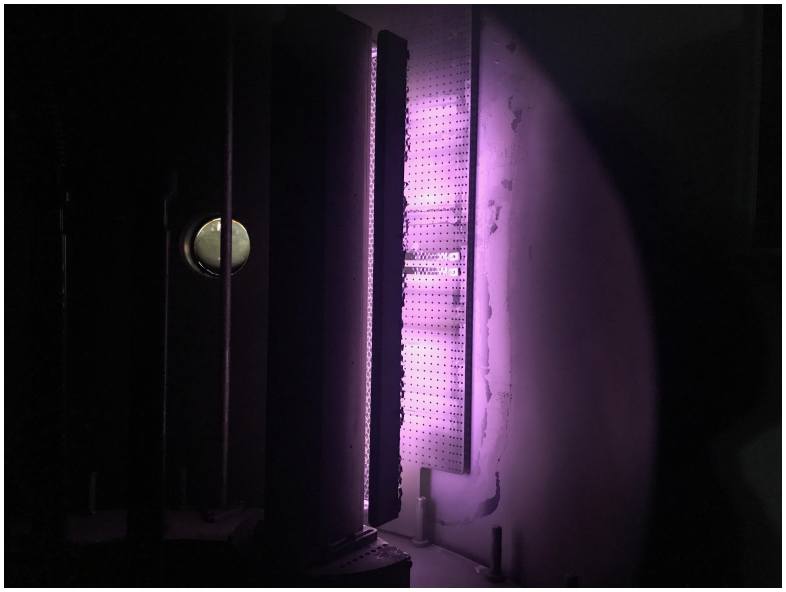

Figure 4: Deposition of iridium films.

3. RESULTS

3.1 Ir and B_4C film composition

The thin film compositions were studied in-depth with XPS measurements and the results were used as a basis for the XRR modelling. The XPS measurements were performed in a Thermo Scientific K-Alpha system allowing for depth profiling analysis with the integrated Ar ion-beam sputter etcher (see measured sample in figure 5). The samples were probed with a monochromized beam (Al K-Alpha: 1486.6 eV) at a take-off angle of 90°. For the non-conductive films, positive charge builds up locally and to minimize the effect charge compensation was performed with an ion gun. The depth analysis of the equipment was $\sim$ 9 nm. The acquired atomic spectra were subtracted with a Shirley background and deconvoluted mainly with Gaussian-Lorentzian curves.

The chemical composition of the Ir film is shown in figure 6. We detected C1s, N1s and O1s on the surface of the Ir film, which we ascribe to hydrocarbons accumulating from the atmosphere. The Ir 4f peak was fitted with a LF(0.6, 1, 50, 150) line-shape with a peak at 61.0 eV. Similar results were obtained for reactively sputtered Ir, indicating no reaction of iridium with nitrogen. The depth profile of non-reactively sputtered iridium is presented in figure 9.

The non-reactively deposited boron carbide film indicates a strong reaction with oxygen and nitrogen after deposition. The numerous chemical bonds shown in figure 7 are likely explained by a highly porous deposited film.
The peak binding energies in the B 1s spectrum indicate stochiometric B_4C measured at 188.4 eV[10,11]. The 189.9 eV and 189.6 eV peaks we assign to a B-C bindings.. In the film surface we observe oxidized boron in two

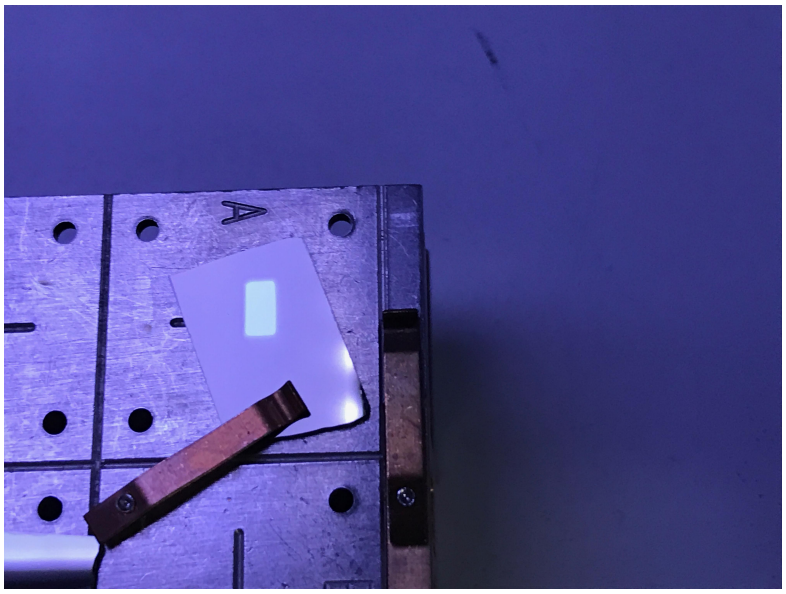

Figure 5: Image of a piece of the coated substrate after XPS measurement. The etched area is indicated as a bright rectangle.

states; we assign the peak at 192.3 eV to boron oxynitride[12], which is likely an intermediate state between boron nitride generally reported at 190.6 eV and boron oxide (B_2O_3) that we observe at 193.6 eV.
The C 1s spectrum was deconvoluted into four component peaks for the film surface and three components for the film interior. Peaks were identified at 283.0 eV, 284.6 eV, 286.4 eV and 288.4 eV. The two lower energies we annotate to B_4C and C-C, respectively, and the two higher energies we assign to C-O and C=O, carbon oxide states[13,14,15]. In the interior of the film, we observe mainly B-C bindings in different states, however no indication of oxidized carbon.
The N 1s energy states are primarily present in the film surface due to atmospheric influence on the film. Literature suggest different chemical states of the binding energy; some propose carbon nitride, others boron nitride and for the highest energy state of 288.4 eV all agree that it is a carbon oxide state. We keep in mind that the atomic concentration of nitrogen is as low as $\sim 2\%$ observed in figure 10.
The peak energies for O 1s are located at 531.8 eV and 532.9-533.0 eV in the film surface as well as the film interior. The latter we ascribe to a C-O chemical state and the former we believe is B_2O_3. The formation of oxide layers on top of thin boron carbide films is well-known and arises from exposure to ambient[16], even at room temperature. A higher concentration of oxygen is observed in the film surface, presented in figure 10. We explain this by a surface saturation of boron oxide and the further diffusion of oxygen into the film is minimized.

The films grown from the reactively sputtered boron carbide target only show one component in the B 1s spectrum with a peak energy at 192.0-192.4 eV (figure 8). Again, we annotate these components to a boron oxynitride state. According to a study performed with RF sputtering of boron nitride films, any residual water or oxide gasses during deposition will affect the stability of the boron nitride films, when exposed to ambient[17]. We derive from this statement that the boron nitride films deposited in our experiment reacted with oxygen into the boron oxynitride state.
Similar to the surface of the non-reactively sputtered boron carbide film we obtain C-N and C-O states in the C 1s, N 1s spectra and O 1s.
The films were only 6-7 nm thick and the peak energy at 532.4 eV is likely originating from the native silicon oxide layer on the substrate.

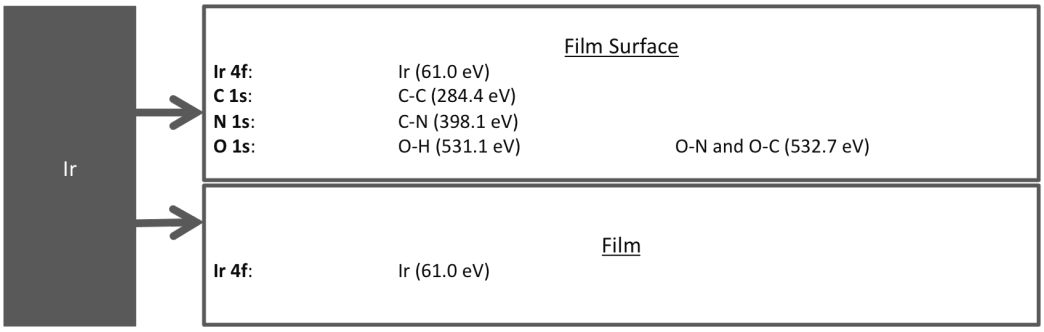

Figure 6: Energy states of non-reactively sputtered iridium film.The Ir 4f spectra was fitted with a LF(0.6,1,50,150) line-shape.

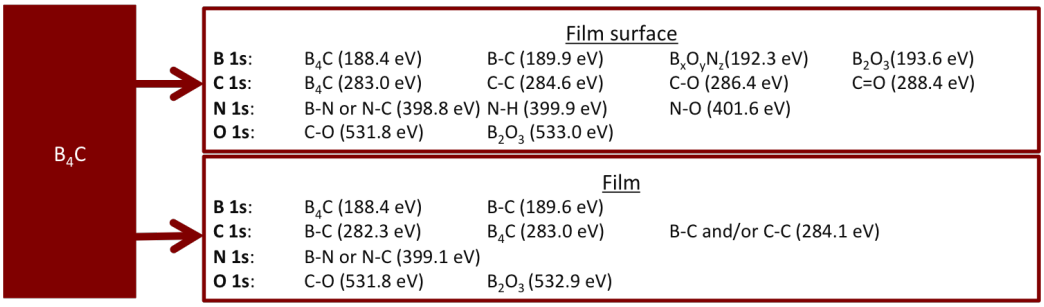

Figure 7: Energy states of non-reactively sputtered boron carbide.

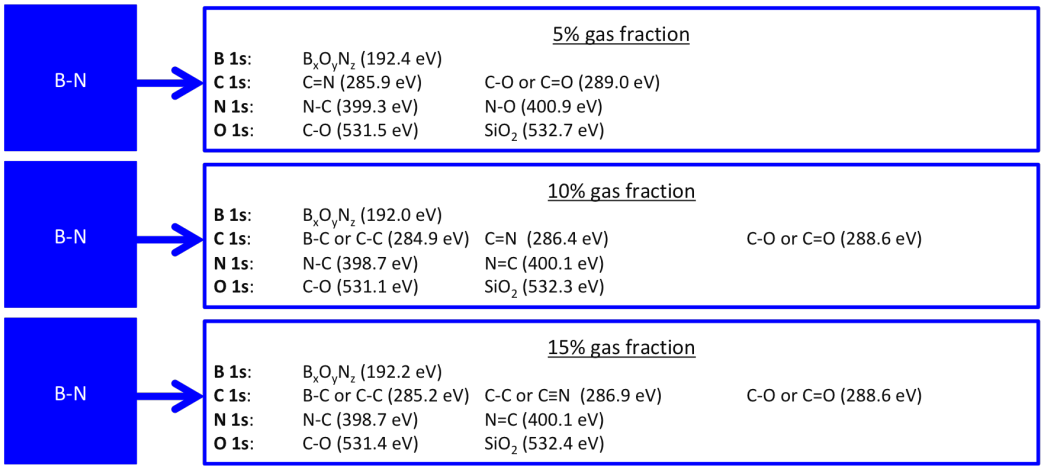

Figure 8: Energy states of the reactively sputtered boron nitride films.

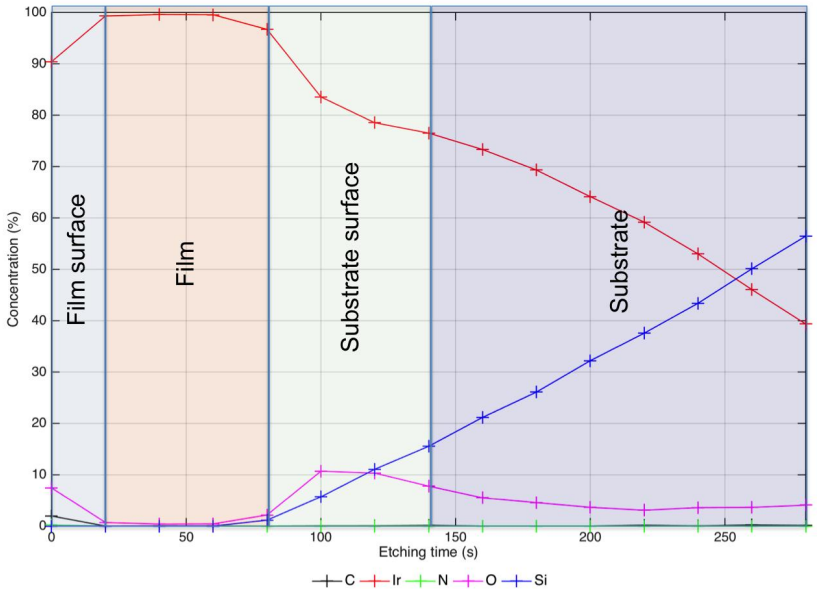

Figure 9: Atomic concentration vs etching time of non-reactively sputtered iridium.

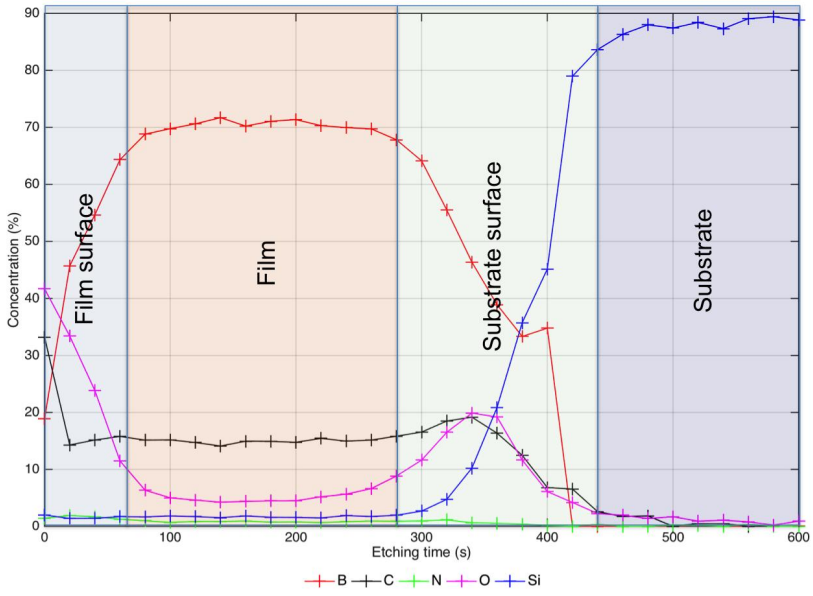

Figure 10: Atomic concentration vs etching time of non-reactively sputtered boron carbide.

3.2 Ir and B_4C film stability

After each deposition we immediately performed 8.047 keV X-ray reflectometry on the samples (setup is described in[18]). Furthermore, we systematically measured the same samples after 7 days, 1 month and several months to identify potential film instabilities.
For iridium films deposited non-reactively and reactively we observe no changes in reflectivity for four measured thicknesses; 4.6 nm, 8.3 nm, 16.7 nm and 25.6 nm. The same is valid for reactively sputtered iridium with thicknesses; 4.4 nm, 8.1 nm, 16.2 nm and 24.5 nm. The reflectivity plots are presented in figures 11 and 12. In addition we do not observe any chemical state time variation for all deposited Ir films.

Figures 13 and 14 show the reflectivity curves of non-reactively and reactively sputtered boron carbide films. Suggested by the results from the XPS measurements, there is a chemical variation in the films and this also shows up in the XRR measurements. We believe the change in reflectivity is caused by a change in film composition as a decrease in film thickness seems unlikely. The best fit models we obtained consisted of a single layer for the very thin films and a double layer for the thicker films. However, the film composition was more complex than the models we were able to create in the software. From XPS measurements we observe a decrease of intensity in the B 1s spectrum and an increase in the C 1s spectrum.

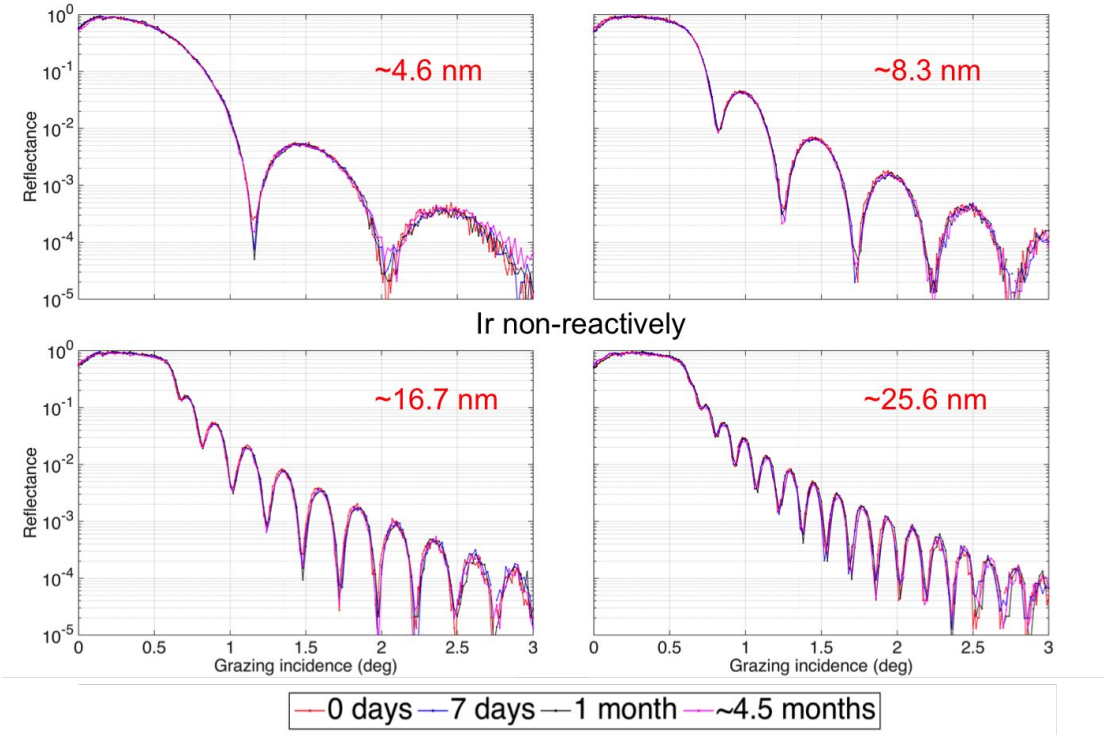

Figure 11: Reflectivity vs grazing incidence.

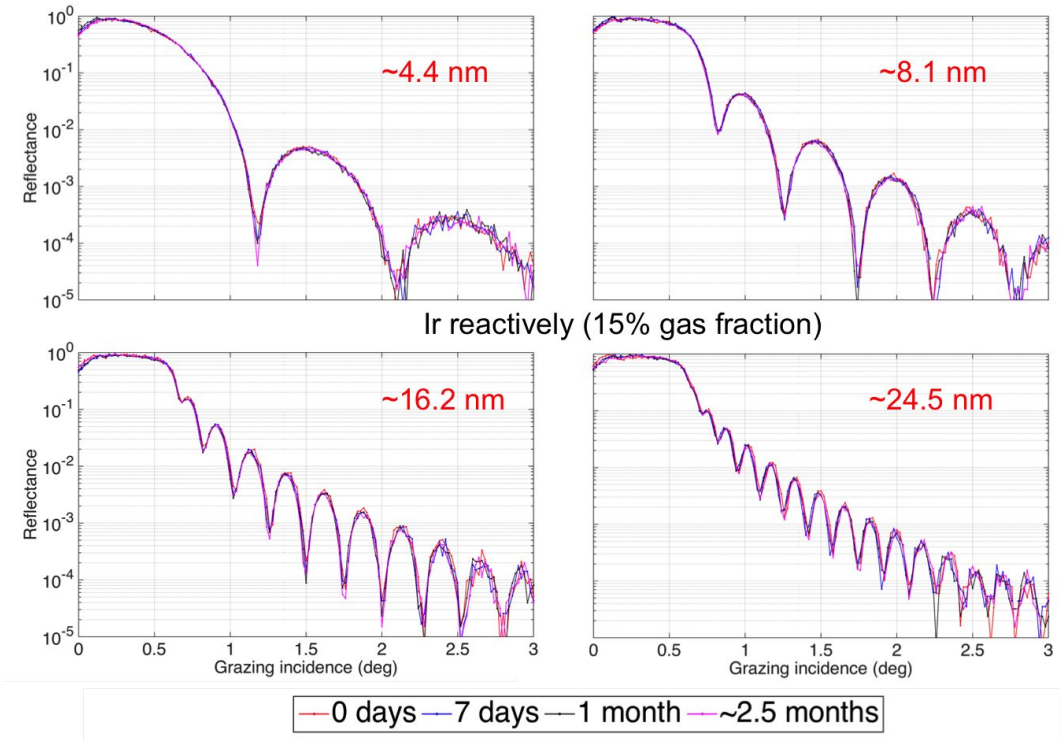

Figure 12: Reflectivity vs grazing incidence.

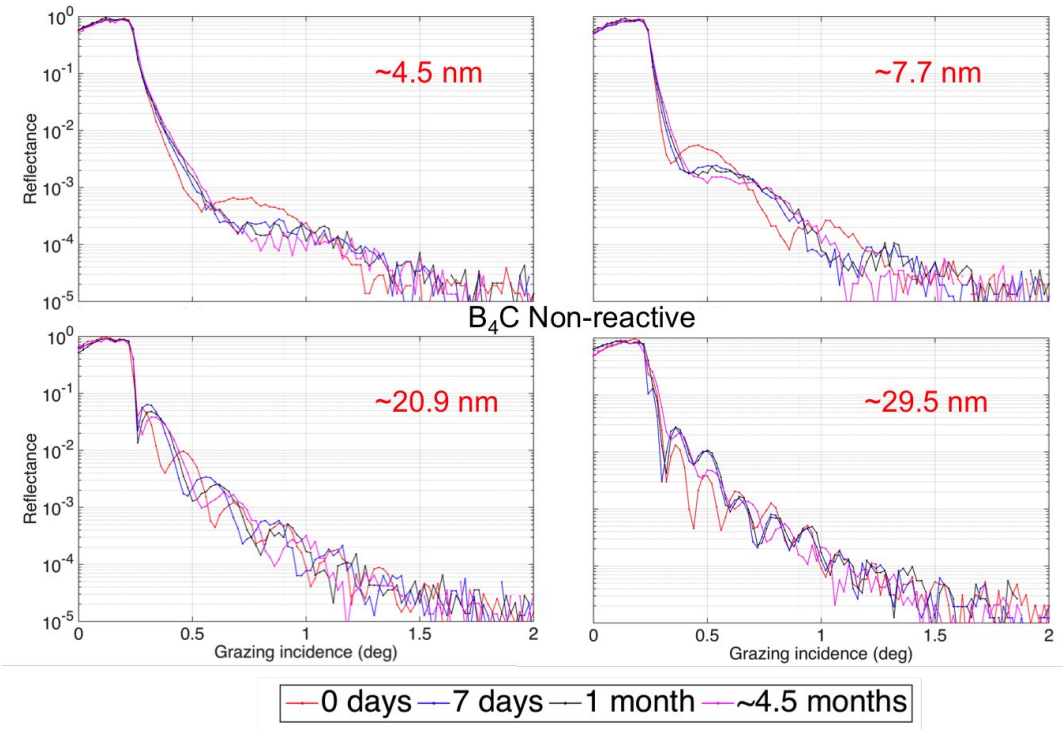

Figure 13: Reflectivity vs grazing incidence.

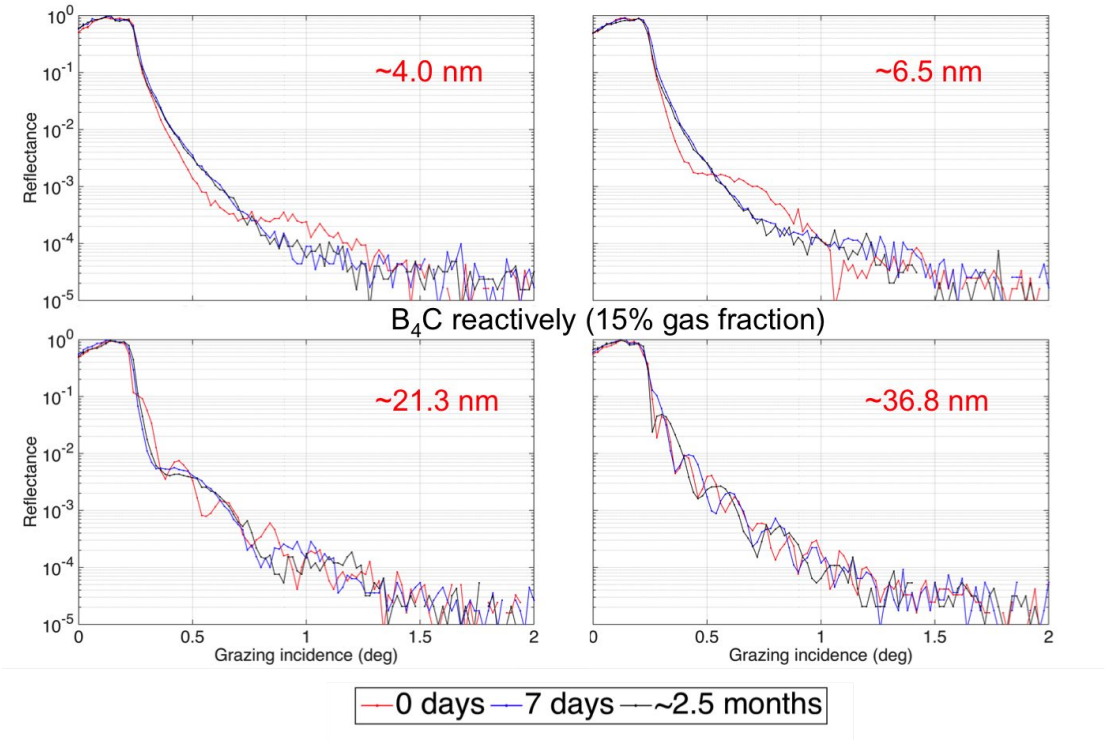

Figure 14: Reflectivity vs grazing incidence.

4. SUMMARY

DC magnetron sputtered iridium films show excellent chemical and reflective properties for X-ray optics. A layer of hydro-carbon originating from ambient conditions is observed on the surface of iridium, which agree with previous studies performed on iridium films. No chemical nor reflectivity changes is observed when we introduced nitrogen in the sputtering process. However, the deposition rate slightly decreased.

The boron carbide films proved chemically unstable when exposed to the ambient. We studied the chemical states of the boron carbide film and observed several B-O and C-O states in the film surface.

The same is valid for reactively sputtered boron carbide, though, we only observed a single component in the B 1s spectrum, which we annotated boron oxynitride. It is still under investigation, whether, the oxygen in the boron nitride film originates from the deposition process or the exposure to ambient conditions after deposition. We did not observe changes in the composition of boron carbide films with respect to gas fraction.

The X-ray reflectivity measurements revealed time-variation of the boron carbide deposited films fortifying the XPS results.

REFERENCES

1. M. Bavdaz, E. Wille, M. Ayre, I. Ferreira, B. Shortt, S. Fransen, M. Collon, G. Vacanti, N. Barriere, B. Landgraf, J. Sforzini, K. Booysen, C. Baren, K. Zuknik, D. Ferreira, S. Massahi, F. Christensen, M. Krumrey, V. Burwitz, G. Pareschi, D. Spiga, G. Valsecchi, D. Vernani, P. Oliver, and A. Seidel, "Development of the athena mirror," *Proceedings of Spie, the International Society for Optical Engineering* , 2018.
2. J. A. Gaskin, R. Allured, S. R. Bandler, S. Basso, M. W. Bautz, M. F. Baysinger, M. P. Biskach, T. M. Boswell, P. D. Capizzo, K.-W. Chan, M. M. Civitani, L. M. Cohen, V. Cotroneo, J. M. Davis, C. T. DeRoo, M. J. DiPirro, A. Dominguez, L. L. Fabisinski, A. D. Falcone, E. Figueroa-Feliciano, J. C. Garcia, K. E. Gelmis, R. K. Heilmann, R. C. Hopkins, T. Jackson, K. Kilaru, R. P. Kraft, T. Liu, R. S. McClelland, R. L. McEntaffer, K. S. McCarley, J. A. Mulqueen, F. Ozel, G. Pareschi, P. B. Reid, R. E. Riveros, M. A. Rodriguez, J. W. Rowe, T. T. Saha, M. L. Schattenburg, A. R. Schnell, D. A. Schwartz, P. M. Solly, R. M.

Suggs, S. G. Sutherlin, D. A. Swartz, S. Trolier-McKinstry, J. H. Tutt, A. Vikhlinin, J. Walker, W. Yoon, and W. W. Zhang, "Lynx observatory and mission concept status," *Proceedings of Spie–the International Society for Optical Engineering* **10397**, p. 103970S, 2017.

3. F. Harrison, D. Stern, D. Alexander, S. Boggs, W. Brandt, L. Brenneman, D. Chakrabarty, F. Christensen, M. Elvis, A. Fabian, N. Gehrels, B. Grefenstette, J. Grindlay, C. Hailey, A. Hornschemeier, A. Hornstrup, V. Kaspi, H. Krawczynski, G. Madejski, K. Madsen, G. Matt, J. Miller, H. Miyasaka, S. Molendi, D. Smith, J. Tomsick, C. Urry, and W. Zhang, "The high-energy x-ray probe (hex-p)," 2016.
4. D. D. M. Ferreira, F. E. Christensen, A. C. Jakobsen, N. J. S. Westergaard, and B. Shortt, "Athena optimized coating design," *Proceedings of Spie, the International Society for Optical Engineering* **8443**, p. 84435L, 2012.
5. D. Della Monica Ferreira, S. Massahi, F. E. Christensen, B. Shortt, M. Bavdaz, M. J. Collon, B. Landgraf, N. C. Gellert, J. Korman, P. Dalampiras, I. F. Rasmussen, I. Kamenidis, M. Krumrey, and S. Schreiber, "Design, development, and performance of x-ray mirror coatings for the athena mission," *Proceedings of Spie 10399* **10399**, pp. 1039918–1039918–10, 2017.
6. D. Della Monica Ferreira, A. C. Jakobsen, S. Massahi, F. E. Christensen, B. Shortt, J. Garnaes, A. Torras-Rosell, M. Krumrey, L. Cibik, and S. Marggraf, "X-ray mirror development and testing for the athena mission," *Proceedings of Space Telescopes and Instrumentation 2016: Ultraviolet To Gamma Ray* **9905**, p. 99055K, 2016.
7. D. Della Monica Ferreira, S. Svendsen, S. Massahi, A. Jafari, L. Vu, J. Korman, N. Gellert, B. Shortt, S. Kadkhodazadeh, T. Kasama, M. Krumrey, and F. Christensen, "Performance and stability of mirror coatings for the athena mission," *Proceedings of Space Telescopes and Instrumentation 2018: Ultraviolet To Gamma Ray* , 2018.
8. D. L. Windt, "Reduction of stress and roughness by reactive sputtering in w/b4c x-ray multilayer films," *Proceedings of Spie–the International Society for Optical Engineering* **6688**, p. 66880R, 2007.
9. S. Massahi, D. A. Girou, D. D. M. Ferreira, F. E. Christensen, A. C. Jakobsen, B. Shortt, M. Collon, and B. Landgraf, "Investigation of photolithography process on spos for the athena mission," *Proceedings of Spie, the International Society for Optical Engineering* **9603**, p. 96030M, 2015.
10. H. Jiang, J. Zhu, Q. Huang, J. Xu, X. Wang, Z. Wang, S. Pfauntsch, and A. Michette, "The influence of residual gas on boron carbide thin films prepared by magnetron sputtering," *Applied Surface Science* **257**(23), pp. 9946–9952, 2011.
11. R. Soufli, A. L. Aquila, F. Salmassi, M. Fernandez-Perea, and E. M. Gullikson, "Optical constants of magnetron-sputtered boron carbide thin films from photoabsorption data in the range 30 to 770 ev," *Applied Optics* **47**(25), pp. 4633–4639, 2008.
12. X. GOUIN, P. GRANGE, L. BOIS, P. L'HARIDON, and Y. LAURENT, "Cheminform abstract: Characterization of the nitridation process of boric acid," *Cheminform* **26**(44), pp. no–no, 2010.
13. Q. Yang, C. B. Wang, S. Zhang, D. M. Zhang, Q. Shen, and L. M. Zhang, "Effect of nitrogen pressure on structure and optical properties of pulsed laser deposited bcn thin films," *Surface and Coatings Technology* **204**(11), pp. 1863–1867, 2010.
14. E. Ech-Chamikh, A. Essafti, Y. Ijdiyaou, and M. Azizan, "Xps study of amorphous carbon nitride (a-c : N) thin films deposited by reactive rf sputtering," *Solar Energy Materials and Solar Cells* **90**(10), pp. 1420–1423, 2006.
15. T. Hu, L. Steihl, W. Rafaniello, T. Fawcett, D. Hawn, J. Mashall, S. Rozeveld, C. Putzig, J. Blackson, W. Cermignani, and M. Robinson, "Structures and properties of disordered boron carbide coatings generated by magnetron sputtering," *Thin Solid Films* **332**(1-2), pp. 80–86, 1998.
16. P. N. Rao, R. K. Gupta, K. Saravanan, A. Bose, S. C. Joshi, T. Ganguli, and S. K. Rai, "Investigation of composition of boron carbide thin films by resonant soft x-ray reflectivity," *Surface and Coatings Technology* **334**, pp. 536–542, 2018.
17. H. Quan, X. Wang, L. Zhang, N. Liu, S. Feng, Z. Chen, L. Hou, Q. Wang, X. Liu, J. Zhao, Y. Gao, and G. Jia, "Stability to moisture of hexagonal boron nitride films deposited on silicon by rf magnetron sputtering," *Thin Solid Films* **642**, pp. 90–95, 2017.

18. S. Massahi, D. Della Monica Ferreira, F. E. Christensen, B. Shortt, D. Girou, M. Collon, B. Landgraf, N. Barriere, M. Krumrey, L. Cibik, and S. Schreiber, "Development and production of a multilayer-coated x-ray reecting stack for the athena mission," *Proceedings of Space Telescopes and Instrumentation 2016: Ultraviolet To Gamma Ray* **9905**, p. 99055P, 2016.